Reset control approximates complex order transfer functions

Valério, Duarte; Saikumar, Niranjan; Dastjerdi, Ali Ahmadi; Karbasizadeh Esfahani, Nima; Hossein Nia Kani, Hassan

DOI
10.1007/s11071-019-05130-2

Publication date
2019

Document Version
Accepted author manuscript

Published in
Nonlinear Dynamics

Citation (APA)
Valério, D., Saikumar, N., Dastjerdi, A. A., Karbasizadeh Esfahani, N., & Hossein Nia Kani, H. (2019). Reset control approximates complex order transfer functions. *Nonlinear Dynamics*, *97*(4), 2323-2337. https://doi.org/10.1007/s11071-019-05130-2

Nonlinear Dynamics manuscript No.
(will be inserted by the editor)

Reset control approximates complex order transfer functions

Duarte Valério * · **Niranjan Saikumar** · **Ali Ahmadi Dastjerdi** · **Nima Karbasizadeh** · **S. Hassan HosseinNia**

Received: date / Accepted: date

Abstract A controller with the frequency response of a complex order derivative may have a gain that decreases with frequency, while the phase increases. This behaviour may be desirable to ensure simultaneous rejection of high frequency noise and robustness to variations of the open loop gain. Implementations of such complex order controllers found in the literature are unsatisfactory for several reasons: the desired behaviour of the gain may be difficult or impossible to obtain, or non-minimum phase zeros may appear, or even unstable open loop poles. We propose an alternative non-linear approximation, combining a CRONE approximation of a fractional derivative with reset control, that does not suffer from these problems. An experimental proof of concept confirms the good results of this approximation, and shows that non-linear effects do not preclude the desired performance.

Keywords Reset control · Fractional calculus · Complex order derivatives · Micro precision

1 Introduction

Fractional order derivatives and integrals have been successfully used to develop controller design techniques with good performances in terms of robustness. Fractional PID control [17] and first and second generation CRONE[1] control [8,10] are examples of such techniques, and already have industrial applications [5].

Fractional Calculus, as is well known, is a misnomer, since the notions of derivative and integral, studied in Calculus, are thereby extended to any non-integer order — which may be fractional, but also irrational, or even complex. Complex order derivatives also have control applications, such as the third generation CRONE control technique [9].

In that technique, the frequency response of a complex derivative is found for the open loop, within the bandwidth of interest; from this desired open loop frequency behaviour, limited in range, and from the frequency behaviour of the plant, a suitable controller is then identified. Thus, the complex derivative is never directly approximated. There are in the literature two attempts to do so. One is the CRONE logarithmic phase controller [7]; the other, a possibly unstable or non-minimum phase implementation [4]. Both have their problems when used in the development of controllers, as detailed below.

This paper proposes approximating the frequency response of a complex derivative combining a CRONE approximation of $s^\alpha, \alpha \in \mathbb{R}^-$ with reset control, which is a non-linear control technique. The advantages and disadvantages of this implementation are discussed, and experimental results are given to show its effectiveness.

The paper addresses, in section 2, the dynamic behaviour of a complex derivative, and shows why published methods to approximate it are inconvenient. Section 3 introduces the proposed approximation, which is

D. Valério (* corresponding author, ORCID 0000-0001-9388-4308)
IDMEC, Instituto Superior Técnico, Universidade de Lisboa, Lisboa, Portugal
E-mail: duarte.valerio@tecnico.ulisboa.pt

N. Saikumar (ORCID 0000-0002-6538-4581), A. A. Dastjerdi, N. Karbasizadeh, S. H. HosseinNia (ORCID 0000-0002-7475-4628)
Department of Precision and Microsystems Engineering, Delft University of Technology, Delft, The Netherlands
E-mail: {n.saikumar, a.ahmadidastjerdi, n.karbasizadehesfahani, s.h.hosseinniakani}@tudelft.nl

[1] CRONE is the French acronym for *non-integer order robust control*.

then shown to be effective in a practical implementation in section 4. Section 5 presents a discussion of the method and of the results and draws conclusions.

2 Frequency response of $s^{\alpha+j\beta}$

There are several possible definitions of a derivative of complex order [16,12,18], usually denoted by operator $D^{\alpha+j\beta}$. For our purpose, it does not matter which one is used, provided that the Laplace transform of a derivative of order $\alpha+j\beta \in \mathbb{C}$ will originate a complex power of the Laplace variable s:

$$\mathscr{L}\left[D^{\alpha+j\beta} f(t)\right] = s^{\alpha+j\beta}\mathscr{L}\left[f(t)\right] \tag{1}$$

It is also irrelevant whether or not terms resulting from initial conditions have to be added to the right hand side of the equality above, or what they are. What is under consideration is the frequency response of the corresponding transfer function $G(s) = s^{\alpha+j\beta}$, the simplest complex order transfer function conceivable. It is given by

$$\begin{aligned} G(j\omega) &= j^{\alpha}\omega^{\alpha} j^{j\beta}\omega^{j\beta} \\ &= \left(\cos\frac{\alpha\pi}{2} + j\sin\frac{\alpha\pi}{2}\right)\omega^{\alpha}\times \\ &\quad \times e^{-\frac{\beta\pi}{2}}\left(\cos(\beta\log\omega) + j\sin(\beta\log\omega)\right) \end{aligned} \tag{2}$$

$$\begin{aligned} 20\log_{10}|G(j\omega)| &= 20\log_{10}\left(\omega^{\alpha}e^{-\frac{\beta\pi}{2}}\right) \\ &= 20\alpha\log_{10}\omega + 20\log_{10}e^{-\frac{\beta\pi}{2}} \end{aligned} \tag{3}$$

$$\begin{aligned} \arg G(j\omega) &= \angle\left\{\left(\cos\frac{\alpha\pi}{2} + j\sin\frac{\alpha\pi}{2}\right)\times\right. \\ &\quad \left.\times\ [\cos(\beta\log\omega) + j\sin(\beta\log\omega)]\right\} \\ &= \frac{\alpha\pi}{2} + \beta\log(10)\log_{10}\omega \end{aligned} \tag{4}$$

The Bode diagram of $G(s)$ is given in Figure 1.

Notice that when $\alpha < 0, \beta > 0$ the gain decreases with frequency, while the phase (and thus the phase margin) increases. This behaviour may be desirable in a controller, inasmuch an increase in the gain of the open-loop, due e.g. to an increase in the gain of the plant, will correspond to a higher gain crossover frequency, at which the controller will have a larger phase margin, thereby likely compensating any decrease of the plant's phase margin. Robustness in presence of plant gain uncertainties can thus be expected (just as in a second generation CRONE controller).

Frequency response (2) can be approximated, for the said case $\alpha < 0$ and $\beta > 0$, in a limited range of frequencies, as proposed in [4], by using a CRONE approximation of s^{α}, described below in section 3.1, replacing the real order α with $-\alpha - j\beta$; the result is a transfer function $\frac{N(s)}{D(s)}$ with a numerator polynomial $N(s)$ and a denominator polynomial $D(s)$ having complex coefficients. The approximation is then obtained as

$$s^{\alpha+j\beta} \approx \frac{D(s) * \bar{D}(s)}{\Re[N(s) * \bar{D}(s)]} \tag{5}$$

where $*$ denotes convolution, and $\bar{D}(s)$ is a polynomial with coefficients that are the complex conjugates of those of $D(s)$. However, [4] indicates that this often leads to either unstable poles or non-minimum phase zeros to appear in the controller, and thus in the control open-loop. This may render this implementation prone to cause an unstable closed-loop when the gain increases or decreases, when robustness to gain variations is precisely what is being sought.

An alternative is the CRONE logarithmic phase controller [7], which has, by construction, only real, stable poles and minimum phase zeros:

$$\tilde{G}(s) = C\prod_{m=1}^{2N}\frac{1+\frac{s}{\omega_{z,m}}}{1+\frac{s}{\omega_{p,m}}} \tag{6}$$

$$\omega_{z,m} = \omega_c\eta^{m-N-\frac{1}{2}} \tag{7}$$

$$\omega_{p,m} = \omega_c\theta^{m-N-\frac{1}{2}} \tag{8}$$

Poles $\omega_{p,m},\ m = 1,\ldots,2N$ and zeros $\omega_{z,m},\ m = 1,\ldots,2N$ are centred on ω_c, and equally spaced in a logarithmic scale of frequencies by recursion coefficients θ and η. The approximation is valid in $[\omega_{p,1},\omega_{p,2N}]\bigcap[\omega_{z,1},\omega_{z,2N}]$, being poor near the limits of this range. Transfer function $\tilde{G}(s)$ has $1/\log_{10}\theta$ poles per decade and $1/\log_{10}\eta$ zeros per decade. The effect of a pole is to decrease the phase by 90°, and the effect of a zero is to increase the phase by 90°, and thus the slope of the phase of $\tilde{G}(s)$ will be $\frac{90^\circ}{\log_{10}\beta} - \frac{90^\circ}{\log_{10}\alpha}$. The phase of $\tilde{G}(s)$ is

$$\arg\tilde{G}(j\omega) = \left(\frac{\pi}{2}\frac{1}{\log_{10}\beta} - \frac{\pi}{2}\frac{1}{\log_{10}\alpha}\right)\log_{10}\omega + \arg\tilde{G}(j\omega)\Big|_{\omega=1} \tag{9}$$

It suffices to choose recursion coefficients θ and η so that $\frac{\pi}{2}\frac{1}{\log_{10}\beta} - \frac{\pi}{2}\frac{1}{\log_{10}\alpha} = \beta\log(10)$ and $\arg\tilde{G}(j\omega)\Big|_{\omega=1} = \frac{\alpha\pi}{2}$ to turn $\tilde{G}(s)$ into an approximation of $G(s) = s^{\alpha+j\beta}$ (cf. the CRONE approximation of s^{α} described in detail in section 3.1 below). Gain $|\tilde{G}(j\omega)|$, however, bears no relation to $|G(j\omega)|$; it may have a positive slope, and consequently it may happen that an increase in the gain of plant will result in the amplification of higher frequencies.

The disadvantages of both these approximations can be overcome using instead the approximation next proposed.

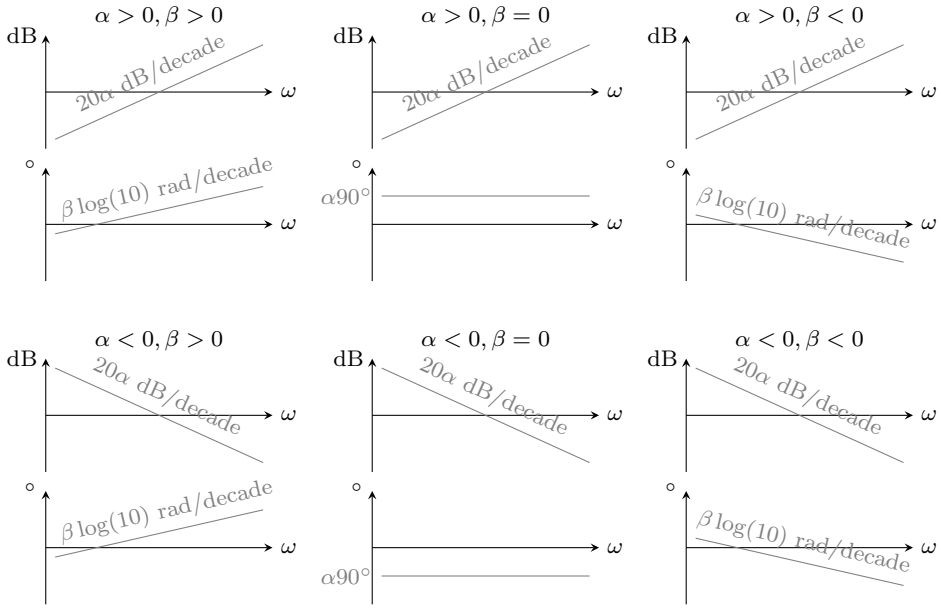

Fig. 1 Bode diagram of $s^{\alpha+j\beta}$.

3 Proposed approximation of $s^{\alpha+j\beta}$

It is possible to approximate $G(s) = s^{\alpha+j\beta}$ combining a CRONE approximation of s^{α} with reset control.

3.1 CRONE approximation of s^{α}

A first generation CRONE controller consists in an approximation of s^{α}, $\alpha \in \mathbb{R}^{-}$, with N real stable poles and N real minimum phase zeros, valid in a limit frequency range $[\omega_l, \omega_h]$, and with α chosen to increase the phase margin of the plant by a suitable value of $90° \times |\alpha|$:

$$s^{\alpha} \approx C \prod_{m=1}^{N} \frac{1 + \frac{s}{\omega_{z,m}}}{1 + \frac{s}{\omega_{p,m}}} \tag{10}$$

$$\omega_{z,m} = \omega_l \left(\frac{\omega_h}{\omega_l}\right)^{\frac{2m-1-\alpha}{2N}} \tag{11}$$

$$\omega_{p,m} = \omega_l \left(\frac{\omega_h}{\omega_l}\right)^{\frac{2m-1+\alpha}{2N}} \tag{12}$$

The correct gain at 1 rad/s, which is $|(j\omega)^{\alpha}| = 1, \ \forall\, \alpha$, must be set by adjusting C. (Using frequency 1 rad/s makes calculations easier, but, if $1 \notin [\omega_l, \omega_h]$, the correct gain at any other suitable frequency will be adjusted instead.)

In practice, this approximation is poor in the half-decade above ω_l and in the half-decade below ω_h but rather good in the rest of the frequency range, provided that there are at least one zero and one pole per decade. The variation of the gain with the logarithm of the frequency is quite close to linearity because each pole lowers the slope of the gain by -20 dB per decade, and each zero increases the slope by $+20$ dB per decade; by construction, poles and zeros alternate in are equally spaced in a logarithmic scale of frequencies, as seen in Figure 2, and if the recursion coefficients δ and ζ are as shown, the average slope of the gain will be $\frac{-20 \log_{10} \delta}{\log_{10} \delta + \log_{10} \zeta}$ dB per decade. The need for at least one zero and one pole per decade is to ensure that ripples will not be significant, and the successive changes in slope merge. As to the phase, it decreases $-90°$ with each pole and increases $+90°$ with each zero, as also seen in Figure 2, and so it remains roughly constant, around a value that depends on the effect of the first zero or pole.

3.2 Reset control

In its simplest form, reset control is a non-linear control technique that consists in setting the output of an integral controller to zero whenever its input is zero. This pole at the origin with reset is known as a Clegg integrator. Figure 3 shows the output of such a controller, $\hat{G}(s) = \frac{1}{s}$, for a sinusoidal input; reset is denoted by an arrow. Since the output never becomes sinusoidal in steady-state, there is no frequency response, but, since it is periodic, it can be studied using a describing function, that considers only the first term of a Fourier series of the output, and neglects all the higher harmonics (which may in some cases be indeed neglectable and

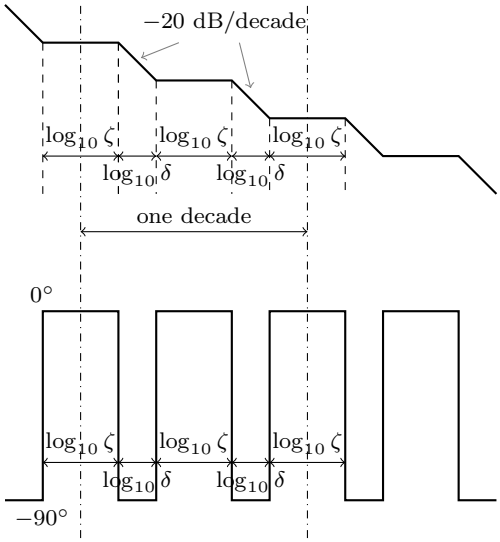

Fig. 2 Bode diagram asymptotes of a CRONE approximation of s^α (adapted from [7]).

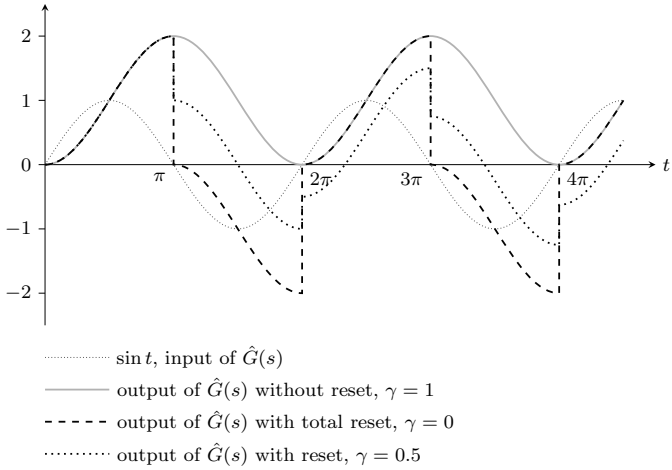

Fig. 3 Response of two reset integrators to a sinusoidal input.

then again may in others not be neglectable at all). It is straightforward to show that [18]

$$20\log_{10}|\hat{G}(j\omega)| = -20\log_{10}\omega + 20\log_{10}\frac{\sqrt{16+\pi^2}}{\pi} \tag{13}$$

$$\arg\hat{G}(j\omega) = -\arctan\frac{\pi}{4} \approx -38^\circ \tag{14}$$

Notice that there is a phase lead of 52° compared to the linear (i.e. without reset) integrator. The slope of the gain is not affected, though the gain is shifted up. (When an integrator is reset in a more complex controller, such as e.g. a first-order filter, this means that the cut-off frequency will change, even though the asymptotic behaviour for both low and high frequencies remains the same.) Figure 3 also shows the output when the reset is not total: rather than the output being set to zero, which is the same as being multiplied by $\gamma = 0$, the output is in this case multiplied by $\gamma = 0.5$. Of course, any other value of the reset coefficient $\gamma \in \mathbb{R}$ could be used, though it is usual to make $-1 \leq \gamma \leq 1$ ($|\gamma| > 1$ risks causing instability). When $\gamma = 1$ there is in fact no reset at all; $\gamma < 0$ causes the sign of the output to be reversed.

In the more general case, reset is applied not directly to the output of a plant, but rather to its N states, there being a different reset coefficient $\gamma_m,\ m = 1,\ldots,N$ for each state. (Of course, if it is in fact the output of the plant that has to be reset, it suffices to use a state-space representation where the output is a state, to set that state's reset coefficient to the desired value, and let all other reset coefficients be 1. The observable canonical form [6] is a possible state-space representation for this purpose.) Reset coefficients are collected in a diagonal matrix $\mathbf{A}_\rho = \mathrm{diag}\,(\gamma_1,\ldots,\gamma_N)$, the reset matrix:

$$\dot{x}(t) = \mathbf{A}x(t) + \mathbf{B}e(t), \qquad \text{if } e(t) \neq 0 \tag{15}$$

$$x(t^+) = \mathbf{A}_\rho x(t), \qquad \text{if } e(t) = 0 \tag{16}$$

$$u(t) = \mathbf{C}x(t) + \mathbf{D}e(t) \tag{17}$$

In this state-space representation of the controller $\hat{G}(t)$, the input is $e(t)$ and $u(t)$ is the controller's output (i.e. the plant's input). It can be shown that the corresponding describing function $\hat{G}(j\omega)$ is given by [3]

$$\hat{G}(j\omega) = \mathbf{C}(j\omega\mathbf{I} - \mathbf{A})^{-1}(\mathbf{I} + j\boldsymbol{\Theta}_\gamma(\omega))\mathbf{B} + \mathbf{D} \tag{18}$$

$$\boldsymbol{\Theta}_\gamma(\omega) = -\frac{2\omega^2}{\pi}\boldsymbol{\Delta}(\omega)\left[\boldsymbol{\Gamma}_\gamma(\omega) - \boldsymbol{\Lambda}^{-1}(\omega)\right] \tag{19}$$

$$\boldsymbol{\Lambda}(\omega) = \omega^2\mathbf{I} + \mathbf{A}^2 \tag{20}$$

$$\boldsymbol{\Delta}(\omega) = \mathbf{I} + e^{\frac{\pi}{\omega}\mathbf{A}} \tag{21}$$

$$\boldsymbol{\Delta}_\gamma(\omega) = \mathbf{I} + \mathbf{A}_\rho e^{\frac{\pi}{\omega}\mathbf{A}} \tag{22}$$

$$\boldsymbol{\Gamma}_\gamma(\omega) = \boldsymbol{\Delta}_\gamma^{-1}(\omega)\mathbf{A}_\rho\boldsymbol{\Delta}(\omega)\boldsymbol{\Lambda}^{-1}(\omega) \tag{23}$$

Notice that if $\mathbf{A}_\rho = \mathbf{I}$ there is no reset, the controller is linear, $\boldsymbol{\Theta}_\gamma(\omega) = \mathbf{0}$, and the usual expression for the transfer function corresponding to a state space is recovered.

With these expressions, it is easy to prove an intuitive result: the smaller phase lag of a Clegg integrator increases as γ is increased from $\gamma = 0$ (total reset) to $\gamma = 1$ (no reset), just as the response is closer to a sinusoid, and thus the weight of higher order harmonics decreases. For $\gamma < 0$ the phase lag decrease is even larger than 52°, but the response is more and more farther from being sinusoidal, and the importance of higher order harmonics increases. Obviously, the farther from linearity a system is, the less the phase margin can be

related to stability, since non-linear effects may suffice to cause instability.

For more details and developments of reset control, see [14,11,2,15].

3.3 Approximating $s^{\alpha+j\beta}$ with alternating zeros and reset poles

If the poles of a first generation CRONE controller (10), that approximates $s^{\alpha'},\ \alpha' < 0$, are reset, then the phase will increase 90° with every zero, but decrease less than 90° with each pole. As a result, it will increase with frequency. At the same time, the asymptotic gain slopes of poles and zeros will not be affected. However, the cut-off frequencies of the reset poles will decrease slightly [13]. The net result is that the gain will still decrease with the frequency. As the system is non-linear, its frequency behaviour must now be studied with a describing function. The asymptotes from which this describing function is to be found are shown in Figure 4.

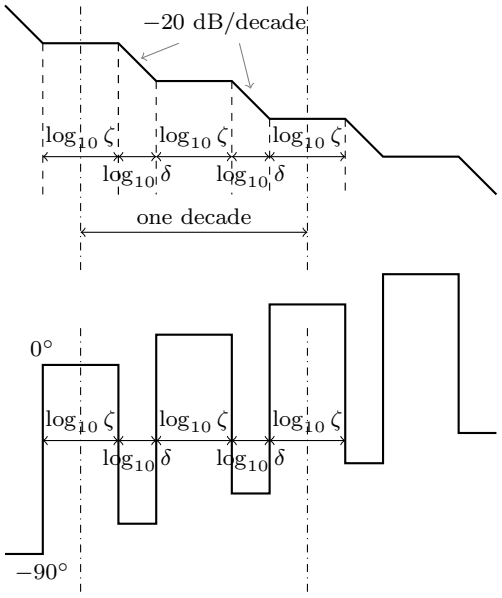

Fig. 4 Describing function asymptotes of the approximation of subsection 3.3 (compare with figure 2).

So this describing function has a phase that increases with frequency, and a gain that decreases with frequency. As seen in Figure 4, because poles and zeros are regularly spaced in a logarithmic scale of frequencies, both gain and phase will be linear in a Bode diagram. Thus, in the frequency range where the approximation is valid, its describing function will approximate the frequency behaviour of $s^{\alpha+j\beta},\ \alpha < 0, \beta > 0$. Notice that the slope of the gain will correspond to a value α which is not the order α' for which the approximation was originally built for, due to the changes of the cut-off frequencies. Also notice that this implementation is an approximation both because it is only valid in a limited frequency range and because it is non-linear. High frequency harmonics may eventually deteriorate its performance.

The transfer function of the approximation described above will be

$$s^{\alpha+j\beta} \approx C \left(\prod_{m=1}^{N} \frac{1}{1+\frac{s}{\omega_{p,m}}}^{\mathbf{A}_\rho} \right) \prod_{m=1}^{N} \frac{1+\frac{s}{\omega_{z,m}}}{1+\frac{s}{\tilde{\omega}_{p,m}}} \tag{24}$$

Notice that, since only the N poles are reset, these have to be implemented separately from the N zeros, which have to remain linear, without any change due to reset. So as to render the linear part of the controller causal, N additional poles $\tilde{\omega}_{p,m},\ m = 1, \ldots, N$ have to be added at high-frequencies (high enough to prevent them from disturbing what happens in the frequency range of interest $[\omega_l, \omega_h]$). The state space representation of the above is

$$\dot{x}_1(t) = \mathbf{A}_1 x_1(t) + \mathbf{B}_1 e(t), \qquad \text{if } e(t) \neq 0 \tag{25}$$
$$x_1(t^+) = \mathbf{A}_\rho x_1(t), \qquad \text{if } e(t) = 0 \tag{26}$$
$$y_1(t) = \mathbf{C}_1 x_1(t) + \mathbf{D}_1 e(t) \tag{27}$$
$$\dot{x}_2(t) = \mathbf{A}_2 x_2(t) + \mathbf{B}_2 y_1(t) \tag{28}$$
$$y_2(t) = \mathbf{C}_2 x_2(t) + \mathbf{D}_2 y_1(t) \tag{29}$$

where matrixes $\mathbf{A}_1, \mathbf{B}_1, \mathbf{C}_1, \mathbf{D}_1$ correspond to the poles of the CRONE approximation which are reset, and matrixes $\mathbf{A}_2$, $\mathbf{B}_2$, $\mathbf{C}_2$, $\mathbf{D}_2$ correspond to the zeros of the CRONE approximation and the high frequencies poles, and thus

$$\left.\frac{y_1(t)}{e(t)}\right|_{\mathbf{A}_\rho=\mathbf{I}} = \mathbf{C}_1 \left(s\mathbf{I} - \mathbf{A}_1\right)^{-1} \mathbf{B}_1 + \mathbf{D}_1 = \prod_{m=1}^{N} \frac{1}{1+\frac{s}{\omega_{p,m}}} \tag{30}$$

$$\frac{y_2(t)}{y_1(t)} = \mathbf{C}_2 \left(s\mathbf{I} - \mathbf{A}_2\right)^{-1} \mathbf{B}_2 + \mathbf{D}_2 = \prod_{m=1}^{N} \frac{1+\frac{s}{\omega_{z,m}}}{1+\frac{s}{\tilde{\omega}_{p,m}}} \tag{31}$$

3.4 Example of the effects

To verify the effect of resetting the poles of a CRONE controller as in (25)–(29), a particular case $\hat{G}(s) \approx s^{-0.5}$ was studied, with $N = 2$ poles and zeros in frequency range $[\omega_l, \omega_h] = [\frac{1}{\sqrt{10}}, 10\sqrt{10}]$ rad/s; the approximation is thus valid in $[1, 10]$ rad/s. The two high-frequency poles are set one decade above ω_h, at $\tilde{\omega}_p =$

$100\sqrt{10}$ rad/s; thus,

$$\hat{G}(s) = \left(\frac{1}{(s+0.56234)(s+5.6234)} \right)^{\mathbf{A}_\rho} \times \times \frac{17783(s+1.7783)(s+17.783)}{(s+316.2)^2} \quad (32)$$

where $\mathbf{A}_\rho = \mathrm{diag}(\gamma_1, \gamma_2)$. Three different state-space representations of the reset poles were tried: the observable, controllable, and diagonal forms, as given by [6]. Figure 5 shows the (average) slope of the gain, the (average) slope of the phase, and the minimum value of the phase, calculated in the $[1, 10]$ rad/s frequency range, using the describing function given by (18)–(23), for the controllable state-space representation, when $-1 \leq \gamma_1, \gamma_2 \leq 1$. (The minimum value of the phase is relevant, since it is undesirable to decrease the phase of the open loop near the crossover frequency.) Similar plots can likewise be found for other state space representations, for values of α other than -0.5, and for other values of $[\omega_l, \omega_h]$. It is to be remarked that the slope of the gain is not always roughly -10 dB/decade, as when there is no reset, but that there are pairs of values γ_1, γ_2 for which that slope is attained, corresponding to different slopes of the phase.

For instance, it can be seen in Figure 5 that, if (32) is to have a gain slope of -20 dB/decade and a phase slope of 20°/decade, it is necessary to make $\gamma_1 \approx 0.8$ and $\gamma_2 \approx -0.6331$. The describing function corresponding to more precise values of γ_1 and γ_2 is shown in Figure 6, together with the desired slopes. It can be seen that the approximation is reasonable in $[1, 10]$ rad/s.

3.5 Tabular method to find a reset controller

The results above suggest a simple method to find a reset controller that approximates $s^{\alpha+j\beta}$ in a frequency range of one decade. For this purpose, several CRONE approximations were built for s^α, $\alpha = -0.1, -0.2, -0.3, \ldots$ with $N = 2$ poles and zeros in frequency range $[\omega_l, \omega_h] = [\frac{1}{\sqrt{10}}, 10\sqrt{10}]$ rad/s. The two high-frequency poles are set at $\tilde{\omega}_p = 100\sqrt{10}$ rad/s again. The effect of varying $-1 \leq \gamma_1, \gamma_2 \leq 1$ was studied and for each approximation the pairs of values γ_1, γ_2 for which the slope of the gain remains equal to $\alpha 90°$ were kept. From the different slopes of the phase obtained, those corresponding to $10°, 15°, 20°, \ldots, 90°$ per decade were tabulated. The results are given in Table 1 when the controllable canonical form is used; similar tables for the observable and diagonal forms are available online as supplementary material for this paper.

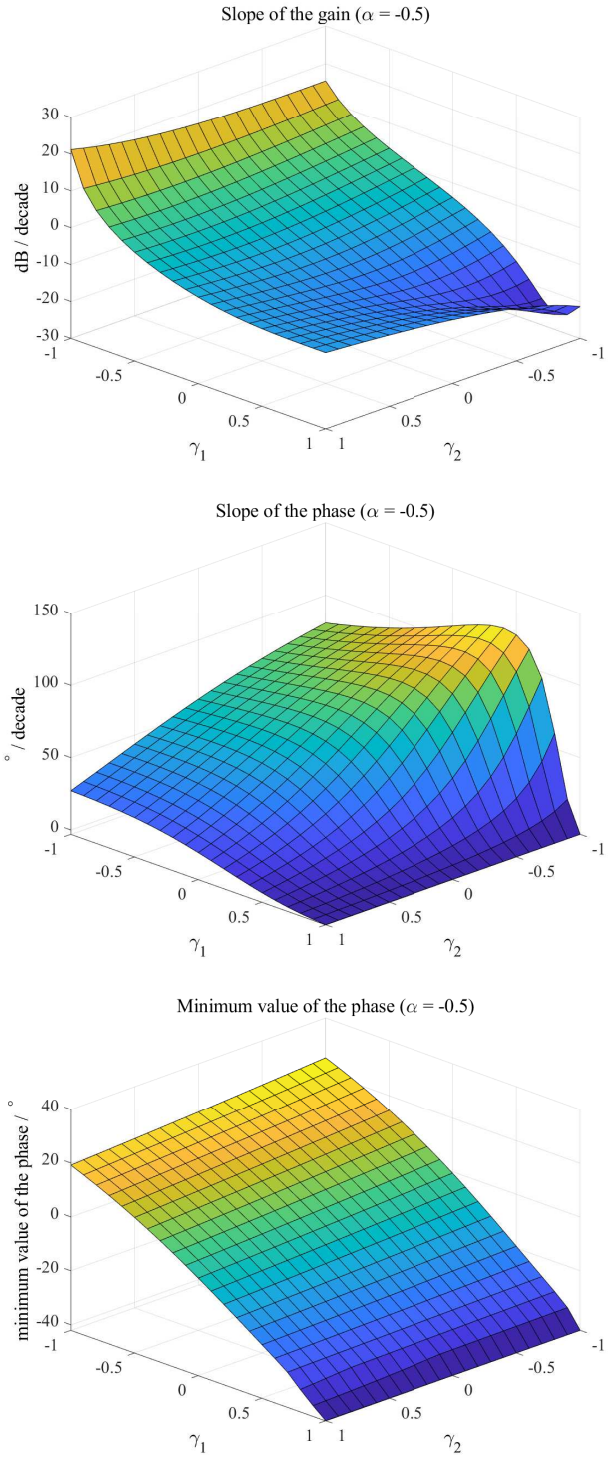

Fig. 5 Slope of the gain (average), slope of the phase (average), and minimum value of the phase, in $[1, 10]$ rad/s, for (32), when the poles are reset as described in section 3.4, using a controllable state-space representation.

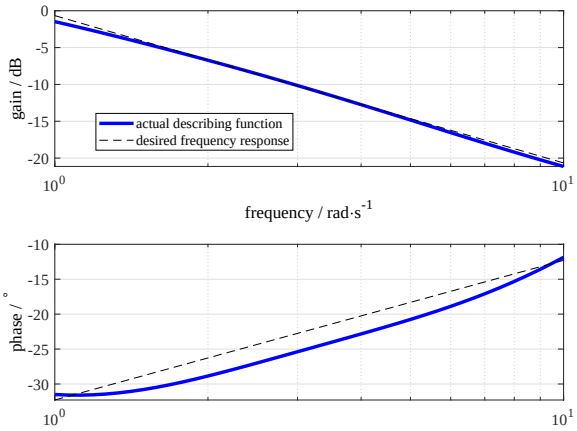

Fig. 6 Describing function of (32) when $\gamma_1 \approx 0.8$, $\gamma_2 \approx -0.6331$, corresponding to a gain slope of of -20 dB/decade and a phase slope of $20°$/decade.

In short, the algorithm to find a controller is as follows:

- Find the desired order of $s^{\alpha+j\beta}$ from the corresponding slopes of gain and phase, per the relations in Figure 1.
- Find a CRONE approximation of s^α, using (10)–(12) with $N = 2$, $\omega_l = \frac{1}{\sqrt{10}}$ rad/s, and $\omega_h = 10\sqrt{10}$ rad/s.
- Convert that approximation into a state space representation given by (25)–(31), using $\tilde{\omega}_p = 100\sqrt{10}$ rad/s, using the controllable (or the observable, or the diagonal) canonical form for the matrixes in (25) and (27).
- Find in Table 1 (or in the tables of the supplementary material for this paper, if the observable or the diagonal canonical forms were used instead of the controllable) the values of γ_1, γ_2, the diagonal elements of $\mathbf{A}_\rho$.
- If the frequency range where the controller should approximate $s^{\alpha+j\beta}$ is not $[1, 10]$ rad/s, multiply all poles and zeros by a suitable constant.

3.6 More general algorithm to find a controller

Using tables to find coefficients is a method with significant disadvantages. First, the frequency range where the approximation is valid is fixed in advance and cannot be changed. Second, this method restricts results to tabulated values, or causes interpolation errors. While such errors cannot be eliminated in the following manner of finding a reset controller that approximates $s^{\alpha+j\beta}$, they are however minimised:

- Find the desired order of $s^{\alpha+j\beta}$ from the corresponding slopes of gain and phase, per the relations in Figure 1.
- Find a CRONE approximation of s^α, using (10)–(12) with $N = 2$ or $N = 3$, and the desired values of ω_l and ω_h. Remember that performance is poor near the limits of the frequency range $[\omega_l, \omega_h]$; consequently, it will only be verified in $[\omega'_l, \omega'_h]$, omitting e.g. half a decade on either side. When $N = 2$, it is difficult to obtain a good approximation if $[\omega'_l, \omega'_h]$ spans more than one decade. When $N = 3$, the approximation holds over two decades.
- Convert that approximation into a state space representation given by (25)–(31), using $\tilde{\omega}_p = 10\omega_h$, using the observable, controllable, or the diagonal canonical form for the matrixes in (25) and (27).
- Find the (average) slope of the gain in $[\omega'_l, \omega'_h]$, when $-1 \le \gamma_1 \le 1$ and $-1 \le \gamma_2 \le 1$ (and, if $N = 3$, also $-1 \le \gamma_3 \le 1$), using some suitable discretisation, e.g. $\gamma_i = -1, -0.95, -0.09, \ldots, 0.95, 1$, $i = 1, 2$ (and 3, if $N = 3$).
- Retain those values of $\mathbf{A}_\rho = \mathrm{diag}(\gamma_i)$ for which the (average) slope of the gain is 20α dB/decade. Find for each of them the (average) slope of the gain in $[\omega'_l, \omega'_h]$, and also the minimum value of the phase in that interval.
- If $N = 2$, there will be only one value of $\mathbf{A}_\rho = \mathrm{diag}(\gamma_1, \gamma_2)$ that has the desired phase: it is the one chosen, and the algorithm ends.
- If $N = 3$, retain the values of $\mathbf{A}_\rho = \mathrm{diag}(\gamma_1, \gamma_2, \gamma_3)$ that have the desired phase. Eliminate those for which the minimum value of the phase in $[\omega'_l, \omega'_h]$ is negative, as we do not want to reduce the phase margin of the open loop. Among the others, that for which gain and phase are closer to linearity (measured e.g. by the quadratic error, and weighting 1 dB of deviation from a linear gain as much as 1° of deviation from a linear phase) is chosen.

This algorithm has been implemented in MATLAB and is available at [1].

When $N > 3$, it is possible to use some numerical minimisation method to find suitable values for γ_i, $i = 1, \ldots, 4$, but results are not more satisfactory than with $N = 3$. In particular, gain and phase are very often far less linear. So, this possibility does not seem very interesting from the practical point of view.

4 Experimental validation

The performance of the approximation of $s^{\alpha+j\beta}$ has been validated experimentally using a precision planar positioning stage. The purpose was not to find the best

Table 1 Values of γ_1 and γ_2 when the controllable canonical form is used in the method of section 3.5.

dB per decade		° per decade																		
		0	**5**	**10**	**15**	**20**	**25**	**30**	**35**	**40**	**45**	**50**	**55**	**60**	**65**	**70**	**75**	**80**	**85**	**90**
−2	γ_1	0.8335	0.6491	0.5212	0.4232	0.3459	0.2840	0.2331	0.1912	0.1571	0.1297	0.1076	0.0907	0.0783	0.0701	0.0656	0.0647	0.0670	0.0725	0.0810
	γ_2	0.9430	0.8972	0.8304	0.7528	0.6697	0.5815	0.4904	0.3970	0.3013	0.2035	0.1040	0.0025	−0.1010	−0.2064	−0.3139	−0.4233	−0.5349	−0.6484	−0.7640
−4	γ_1	0.8167	0.6273	0.4982	0.4025	0.3285	0.2694	0.2217	0.1831	0.1518	0.1276	0.1087	0.0948	0.0854	0.0801	0.0784	0.0802	0.0853	0.0935	0.1044
	γ_2	0.9000	0.8594	0.7967	0.7234	0.6434	0.5603	0.4745	0.3866	0.2973	0.2057	0.1130	0.0187	−0.0773	−0.1748	−0.2739	−0.3746	−0.4768	−0.5807	−0.6860
−6	γ_1	0.7985	0.6027	0.4752	0.3812	0.3097	0.2531	0.2089	0.1738	0.1456	0.1245	0.1087	0.0977	0.0913	0.0888	0.0901	0.0947	0.1026	0.1132	0.1265
	γ_2	0.8628	0.8278	0.7679	0.6973	0.6219	0.5428	0.4611	0.3777	0.2934	0.2073	0.1204	0.0322	−0.0573	−0.1480	−0.2399	−0.3330	−0.4272	−0.5226	−0.6189
−8	γ_1	0.7789	0.5768	0.4489	0.3580	0.2892	0.2366	0.1946	0.1630	0.1383	0.1201	0.1074	0.0995	0.0961	0.0967	0.1009	0.1083	0.1188	0.1320	0.1480
	γ_2	0.8307	0.8010	0.7446	0.6767	0.6034	0.5274	0.4496	0.3701	0.2897	0.2083	0.1262	0.0432	−0.0409	−0.1258	−0.2115	−0.2981	−0.3854	−0.4734	−0.5619
−10	γ_1	0.7552	0.5480	0.4222	0.3330	0.2675	0.2178	0.1797	0.1503	0.1296	0.1146	0.1052	0.1003	0.1003	0.1039	0.1111	0.1214	0.1345	0.1506	0.1685
	γ_2	0.8046	0.7810	0.7254	0.6590	0.5879	0.5142	0.4390	0.3631	0.2857	0.2081	0.1300	0.0512	−0.0283	−0.1083	−0.1887	−0.2697	−0.3510	−0.4327	−0.5144
−12	γ_1	0.7294	0.5175	0.3916	0.3055	0.2434	0.1967	0.1630	0.1374	0.1200	0.1082	0.1023	0.1010	0.1042	0.1110	0.1213	0.1344	0.1507	0.1687	0.1894
	γ_2	0.7836	0.7646	0.7101	0.6447	0.5748	0.5027	0.4292	0.3553	0.2809	0.2063	0.1313	0.0560	−0.0196	−0.0955	−0.1715	−0.2476	−0.3238	−0.3998	−0.4757
−14	γ_1	0.6988	0.4832	0.3596	0.2778	0.2188	0.1761	0.1450	0.1237	0.1099	0.1018	0.0997	0.1020	0.1087	0.1189	0.1322	0.1488	0.1672	0.1883	0.2110
	γ_2	0.7673	0.7515	0.6970	0.6316	0.5620	0.4907	0.4190	0.3466	0.2743	0.2020	0.1296	0.0571	−0.0153	−0.0876	−0.1598	−0.2318	−0.3034	−0.3746	−0.4454
−16	γ_1	0.6666	0.4471	0.3272	0.2471	0.1925	0.1542	0.1280	0.1107	0.1004	0.0967	0.0986	0.1047	0.1151	0.1287	0.1454	0.1647	0.1862	0.2096	0.2345
	γ_2	0.7514	0.7405	0.6846	0.6187	0.5489	0.4782	0.4069	0.3360	0.2652	0.1946	0.1242	0.0541	−0.0156	−0.0849	−0.1538	−0.2221	−0.2898	−0.3569	−0.4230
−18	γ_1	0.6334	0.4116	0.2935	0.2189	0.1691	0.1349	0.1126	0.0994	0.0938	0.0947	0.1005	0.1106	0.1248	0.1421	0.1620	0.1843	0.2086	0.2340	0.2608
	γ_2	0.7340	0.7274	0.6707	0.6033	0.5335	0.4629	0.3923	0.3222	0.2525	0.1833	0.1145	0.0465	−0.0209	−0.0876	−0.1535	−0.2186	−0.2828	−0.3460	−0.4082
−20	γ_1	0.6019	0.3791	0.2640	0.1936	0.1474	0.1188	0.1011	0.0929	0.0923	0.0974	0.1074	0.1220	0.1399	0.1605	0.1837	0.2088	0.2352	0.2627	0.2908
	γ_2	0.7081	0.7091	0.6520	0.5848	0.5146	0.4437	0.3737	0.3041	0.2353	0.1673	0.1001	0.0338	−0.0315	−0.0959	−0.1591	−0.2212	−0.2821	−0.3419	−0.4004
−22	γ_1	0.5820	0.3530	0.2418	0.1758	0.1347	0.1103	0.0970	0.0942	0.0979	0.1076	0.1224	0.1407	0.1620	0.1861	0.2120	0.2393	0.2674	0.2965	0.3250
	γ_2	0.6604	0.6817	0.6267	0.5593	0.4894	0.4192	0.3496	0.2807	0.2128	0.1458	0.0801	0.0155	−0.0479	−0.1099	−0.1705	−0.2298	−0.2877	−0.3442	−0.3992
−24	γ_1	0.5815	0.3435	0.2335	0.1706	0.1327	0.1129	0.1049	0.1058	0.1148	0.1288	0.1470	0.1691	0.1940	0.2201	0.2485	0.2766	0.3061	0.3352	0.3644
	γ_2	0.5743	0.6368	0.5890	0.5246	0.4561	0.3869	0.3182	0.2502	0.1833	0.1178	0.0536	−0.0091	−0.0705	−0.1299	−0.1883	−0.2445	−0.2995	−0.3527	−0.4044
−26	γ_1	0.6147	0.3583	0.2443	0.1835	0.1475	0.1319	0.1285	0.1335	0.1454	0.1632	0.1848	0.2093	0.2356	0.2636	0.2929	0.3216	0.3517	0.3798	0.4086
	γ_2	0.4160	0.5636	0.5336	0.4757	0.4112	0.3440	0.2770	0.2108	0.1457	0.0820	0.0198	−0.0410	−0.0997	−0.1568	−0.2123	−0.2655	−0.3177	−0.3673	−0.4159
−28	γ_1	0.6893	0.4098	0.2865	0.2220	0.1874	0.1738	0.1722	0.1796	0.1937	0.2135	0.2365	0.2620	0.2889	0.3169	0.3453	0.3733	0.4023	0.4290	0.4568
	γ_2	0.1465	0.4413	0.4477	0.4049	0.3483	0.2861	0.2229	0.1597	0.0974	0.0364	−0.0230	−0.0809	−0.1367	−0.1908	−0.2430	−0.2931	−0.3421	−0.3883	−0.4338
−30	γ_1	0.7816	0.5056	0.3676	0.2942	0.2586	0.2415	0.2390	0.2466	0.2613	0.2804	0.3032	0.3268	0.3532	0.3785	0.4058	0.4311	0.4576	0.4824	0.5072
	γ_2	−0.1918	0.2405	0.3137	0.3010	0.2586	0.2070	0.1507	0.0929	0.0353	−0.0215	−0.0775	−0.1306	−0.1834	−0.2328	−0.2818	−0.3278	−0.3730	−0.4159	−0.4576
−32	γ_1	0.8558	0.6346	0.4871	0.4033	0.3618	0.3382	0.3320	0.3356	0.3456	0.3621	0.3809	0.4022	0.4240	0.4477	0.4698	0.4939	0.5155	0.5375	0.5599
	γ_2	−0.4796	−0.0501	0.1115	0.1468	0.1294	0.0967	0.0526	0.0048	−0.0443	−0.0949	−0.1441	−0.1927	−0.2391	−0.2851	−0.3280	−0.3710	−0.4109	−0.4500	−0.4881
−34	γ_1	0.9048	0.7493	0.6256	0.5376	0.4872	0.4547	0.4442	0.4398	0.4436	0.4543	0.4682	0.4837	0.5006	0.5194	0.5375	0.5570	0.5754	0.5938	0.6119
	γ_2	−0.6773	−0.3428	−0.1538	−0.0652	−0.0442	−0.0489	−0.0758	−0.1080	−0.1449	−0.1857	−0.2265	−0.2668	−0.3066	−0.3462	−0.3835	−0.4209	−0.4563	−0.4907	−0.5238
−36	γ_1	0.9322	0.8326	0.7407	0.6680	0.6159	0.5835	0.5618	0.5475	0.5463	0.5482	0.5568	0.5687	0.5797	0.5924	0.6058	0.6201	0.6348	0.6503	0.6636
	γ_2	−0.7916	−0.5739	−0.4066	−0.3041	−0.2510	−0.2337	−0.2333	−0.2419	−0.2651	−0.2908	−0.3221	−0.3554	−0.3859	−0.4171	−0.4481	−0.4784	−0.5087	−0.5387	−0.5659
−38	γ_1	0.9542	0.8838	0.8210	0.7675	0.7270	0.6905	0.6721	0.6490	0.6438	0.6435	0.6444	0.6453	0.6542	0.6659	0.6739	0.6819	0.6922	0.7035	0.7142
	γ_2	−0.8791	−0.7222	−0.5997	−0.5109	−0.4558	−0.4129	−0.4033	−0.3871	−0.3978	−0.4133	−0.4301	−0.4469	−0.4721	−0.4997	−0.5216	−0.5434	−0.5669	−0.5912	−0.6139

possible controller for this plant, but rather to use it as a proof of concept for the desirable characteristics of this non-linear approximation of a complex order controller.

4.1 The three-degree-of-freedom planar precision "Spyder" stage

The precision planar positioning stage used for performance validation is shown in Figure 7. Since SISO controllers are being designed, only one of the actuators (the one marked as 1A) was used, for position control of mass number 3 attached to same actuator, thus resulting in a SISO system. LM388 power amplifier is used to power the actuator with position feedback of resolution 100 nm, obtained through a Mercury M2000 linear encoder placed under the mass 3. A chirp signal was applied to the system, and the frequency response obtained is shown in Figure 8. From this frequency response, the following transfer function model can be found using Levy's method [14]:

$$G(s) = \frac{5.049 \times 10^4}{s^2 + 48.05s + 7421} \tag{33}$$

A complex order controller was designed for this system for crossover frequency of 75 Hz (471.2 rad/s), according to the details provided in the next subsection.

4.2 The controllers

The complex order controller designed for the crossover frequency of 75 Hz (471.2 rad/s) includes an approximation $\hat{G}(s) \approx s^{-0.5+j0.6064}$, thus corresponding to a

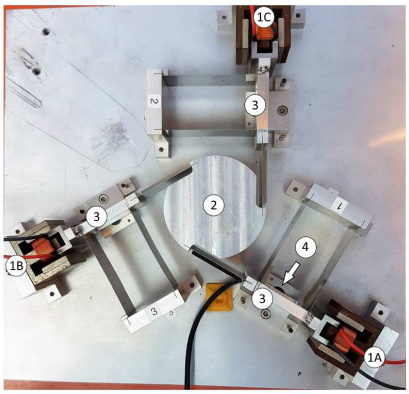

Fig. 7 A precision planar positioning stage named 'Spyder'. 3 masses (indicated by the number 3) are actuated by voice coil actuators 1A, 1B and 1C. These masses are constrained using leaf flexures with additional flexures connecting them to the central mass (indicated by 2). Position feedback is provided by linear encoders (indicated by 4) placed under the masses labelled with number 3.

−10 dB/decade slope of the gain, and a 80°/decade slope of the phase. This approximation uses the controllable canonical form, with $N = 2$ poles and zeros in the $[23.5, 2356]$ rad/s frequency range, being thus expected to be a good approximation in the $[74.5, 745]$ rad/s frequency range. The high frequency poles used to ensure causality of the linear part are placed at 10 times the crossover frequency, i.e. at 4712 rad/s. A PI controller is also concatenated to $\hat{G}(s)$, to improve tracking performance at low frequencies. The overall designed con-

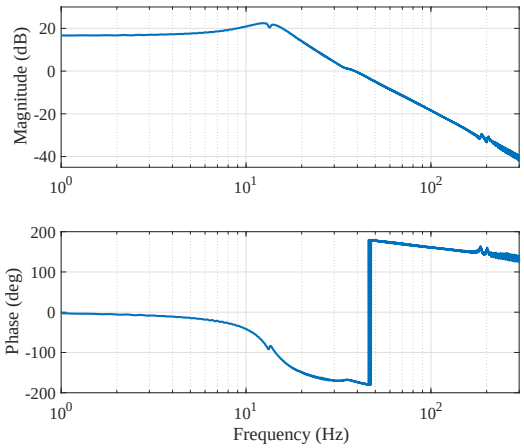

Fig. 8 Frequency response data of the system. Input: actuator 1A. Output: position of mass 3 attached to the same actuator.

troller is given by

$$C_1(s) = \hat{G}(s)\frac{4.6202\times 10^7(s+47.12)}{s}\frac{(s+1325)(s+132.5)}{(s+4712)^2} \tag{34}$$

where

$$\hat{G}(s) = \left(\frac{1}{(s+41.9)(s+419)}\right)^{\mathbf{A}_\rho} \tag{35}$$

with

$$\mathbf{A}_\rho = \begin{bmatrix} -0.351 & 0 \\ 0 & 0.1345 \end{bmatrix} \tag{36}$$

As a term of comparison, the following PID controller was also designed for the same bandwidth, and also ensuring the same phase margin is achieved by both controllers:

$$C_2(s) = \frac{2.5708\times 10^9(s+174)(s+47.12)}{s(s+4.712\times 10^4)(s+4712)(s+1276)} \tag{37}$$

An experimental comparison with approximations obtained with the methods from section 2 will not be presented, because from the approximations of $s^{-0.5+j0.6064}$ got with those methods no good results can be expected. An approximation obtained with (5) has four zeros and four poles; one of the poles is unstable. A reasonable approximation obtained with (6) must have at least six zeros and six poles, and still its performance is poor. Compare this with the two (reset) poles of (35). This is supported by Figure 9 that shows the Bode diagrams of the two approximations obtained with (5) and (6), together with the describing function of the reset approximation used to build (34).

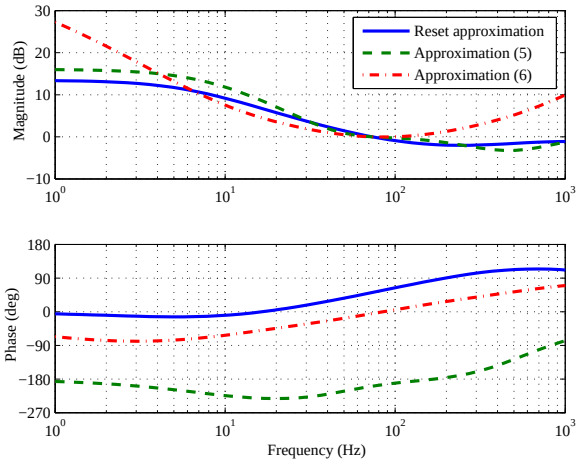

Fig. 9 Describing function of the reset approximation of $s^{-0.5+j0.6064}$ used to build (34), and Bode diagrams of the corresponding approximations (5) and (6); gains were adjusted so that at bandwidth frequency 75 Hz all approximations have gain 0 dB.

Figure 10 compares the open loop with controller (34), found with (18)–(23), with the open loop with controller (37), showing that the phase margin is, indeed, the same. The effect of the positive slope of the phase of the controller in the frequency range of design can also be seen in this figure.

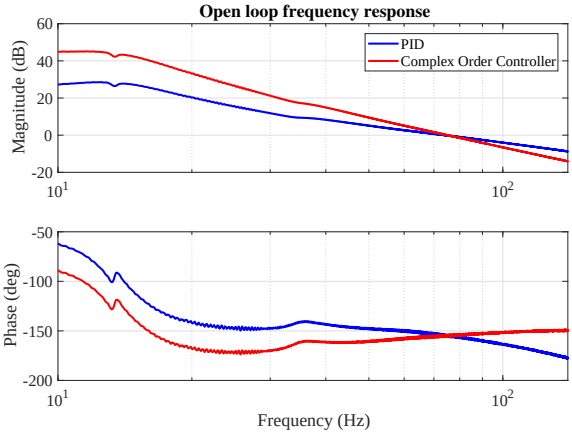

Fig. 10 Open loop frequency response with both controllers. Obtained using describing function of controller (34) and Bode diagram of PID (37).

Both the controllers are discretised for a sampling frequency of 20 kHz for implementation.

The next two sections present experiments to validate the complex order controller. Its main characteristics we wish to verify are: positive phase slope in the region of cross over frequency, negative gain slope in the same region and the extent to which higher order

harmonics affect performance in closed-loop. Step sponses obtained with system gain deviations are us to verify the first and third; closed loop frequency sponses are obtained to verify the first; finally, nc attenuation performance is checked for the second a third characteristics.

4.3 Experimental step responses

The step response for both controllers is obtained the precision positioning stage for a displacement st of 10 μm and shown in Figure 11. Although the controllers are designed to have the same phase margin, as shown in Figure 10, the overshoot of the complex order controller is less than that of the PID.

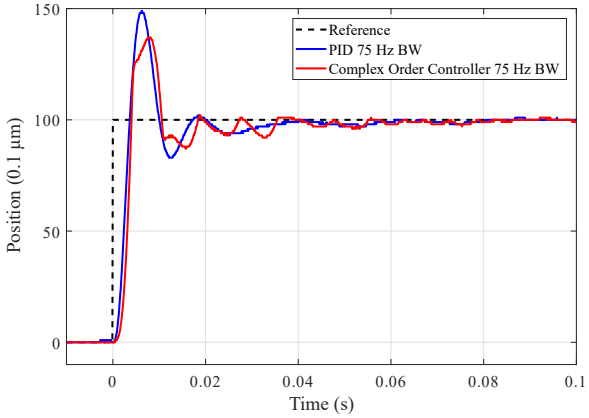

Fig. 11 Step response obtained for both controllers

Furthermore, to validate the concept of robustness to gain variations (which should result from an increased phase margin for an increased system gain, in the case of the complex order controller, as seen in Figure 10), the gain of the system was increased so that the new crossover frequency is 100 Hz. Since all other controller parameters remain unchanged, this results in an increased phase margin compared to the value at 75 Hz. The controller gain was then decreased to obtain a bandwidth of 55 Hz, resulting in a decreased phase margin. These changes in gain were also carried out for the designed PID controller. However, in the case of the PID, increasing the crossover frequency results in a reduced phase margin and vice-versa. The step responses obtained in all the cases are shown in Figure 12.

The responses validate the complex order controller behaviour, since the step response achieved at higher crossover frequency results in a faster response, but with lesser overshoot, indicating an increase in the phase

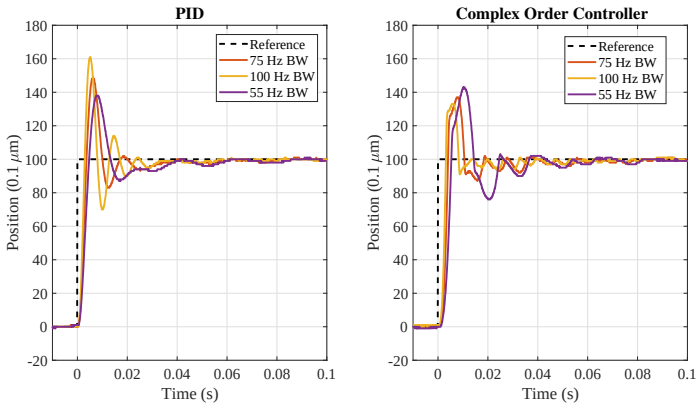

Fig. 12 Step response of both controllers compared for changes in bandwidth

margin of the system, while the opposite is true for reduced crossover frequency. It also validates the use of describing function for both design and analysis of the complex order controller behaviour achieved through the nonlinear reset technique. The step responses of PID are as expected from linear control theory.

4.4 Experimental frequency responses

The closed loop complementary sensitivity responses are obtained for both the controllers at all three crossover frequency values by applying a chirp reference. The obtained plots, shown in Figure 13, further validate the concept of complex order behaviour realised through reset. In the case of PID, an increase in bandwidth results in a decrease in the phase margin and this is directly seen in the complementary sensitivity as an increase in peak. The opposite is true in the case of complex order controller, for which a decrease in peak is seen.

4.5 Experimental responses in the presence of noise

The use of reset to achieve complex order behaviour results in the introduction of higher order harmonics which are not considered in the design or analysis of the controllers. These harmonics may have negative effects on control performance especially in the case of precision systems. This is especially true in the case of noise attenuation which needs to be achieved for higher frequency signals. To study the noise attenuation properties of the closed loop system, and verify if it corresponds to the desired frequency behaviour or if this is prevented by high frequency harmonics, white noise with a maximum amplitude of 5 μm is added into the sensor signal. This is done for both PID and complex

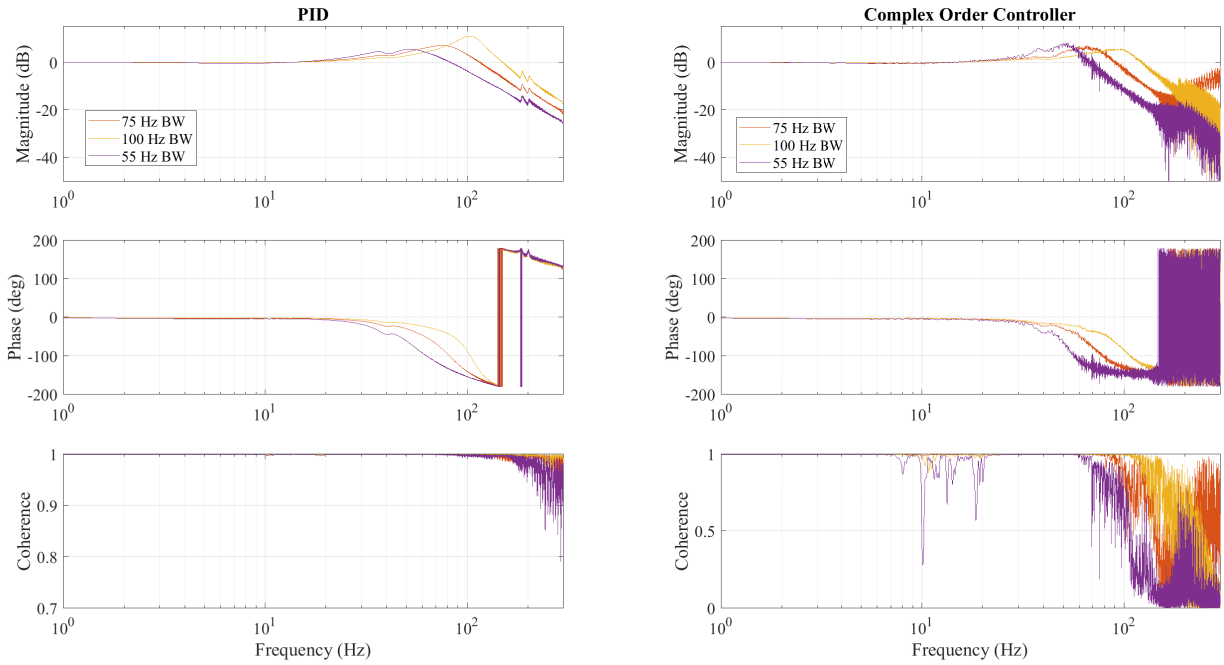

Fig. 13 Closed loop complementary sensitivity for designed PID and complex order controllers. The coherence value is also plotted to show the reliability of obtained responses.

order controller, and for the three different bandwidths. The resulting system response is shown in Figure 14.

The noise attenuation and hence steady state precision achieved in the presence of noise is significantly better for complex order controller compared to PID. Furthermore, in the case of PID, an increase in bandwidth results in higher gain at higher frequencies and hence reduced noise attenuation and vice-versa as seen in the same figure. However, in the case of the complex order controller, due to the nonlinear nature of reset control used, no significant difference is seen in the noise attenuation for different bandwidth values, although the precision achieved is better than that of the PID in all cases. Finally, from these results it is apparent that the higher order harmonics present when reset control is used do not have a negative influence on noise attenuation.

5 Discussion and conclusions

Experimental results confirm that it is possible to implement a stable, non-linear controller, that approximates, in a desired range of frequencies, the behaviour of a complex derivative $s^{\alpha+j\beta}$, $\alpha < 0, \beta > 0$. The frequency response of this complex derivative has the gain decreasing with frequency, while the phase increases. This additional phase lead provides at the same time rejection of high frequency noise and lower overshoots in time responses when the open-loop gain increases. The describing function of the proposed non-linear approximation is close to the desired frequency response over more than one or two decades, depending on the number of reset poles employed. Larger frequency ranges were not obtained because of numerical problems.

An experimental proof of concept, using a precision planar positioning stage, confirmed the usefulness and correctness of the expected results. What is more, these experimental results show that the effects of higher harmonics, resulting from the non-linearity of the controller, and not considered by the describing function approach, do not perturb the expected behaviour, be it of the frequency responses, or of the time responses and the corresponding overshoot, or of noise rejection.

The proposed approximation of a complex order derivative overcomes the shortcomings of the alternatives found in the literature, that either approximate the desired phase behaviour but not the desired gain behaviour, or run the risk of having non-minimum phase zeros or even unstable poles, both undesirable in a control loop.

While the experimental results were obtained solely as a proof of concept, we expect in the future to be able to develop high-performing controllers for industrial problems where the specifications correspond to those that can be obtained with complex order control.

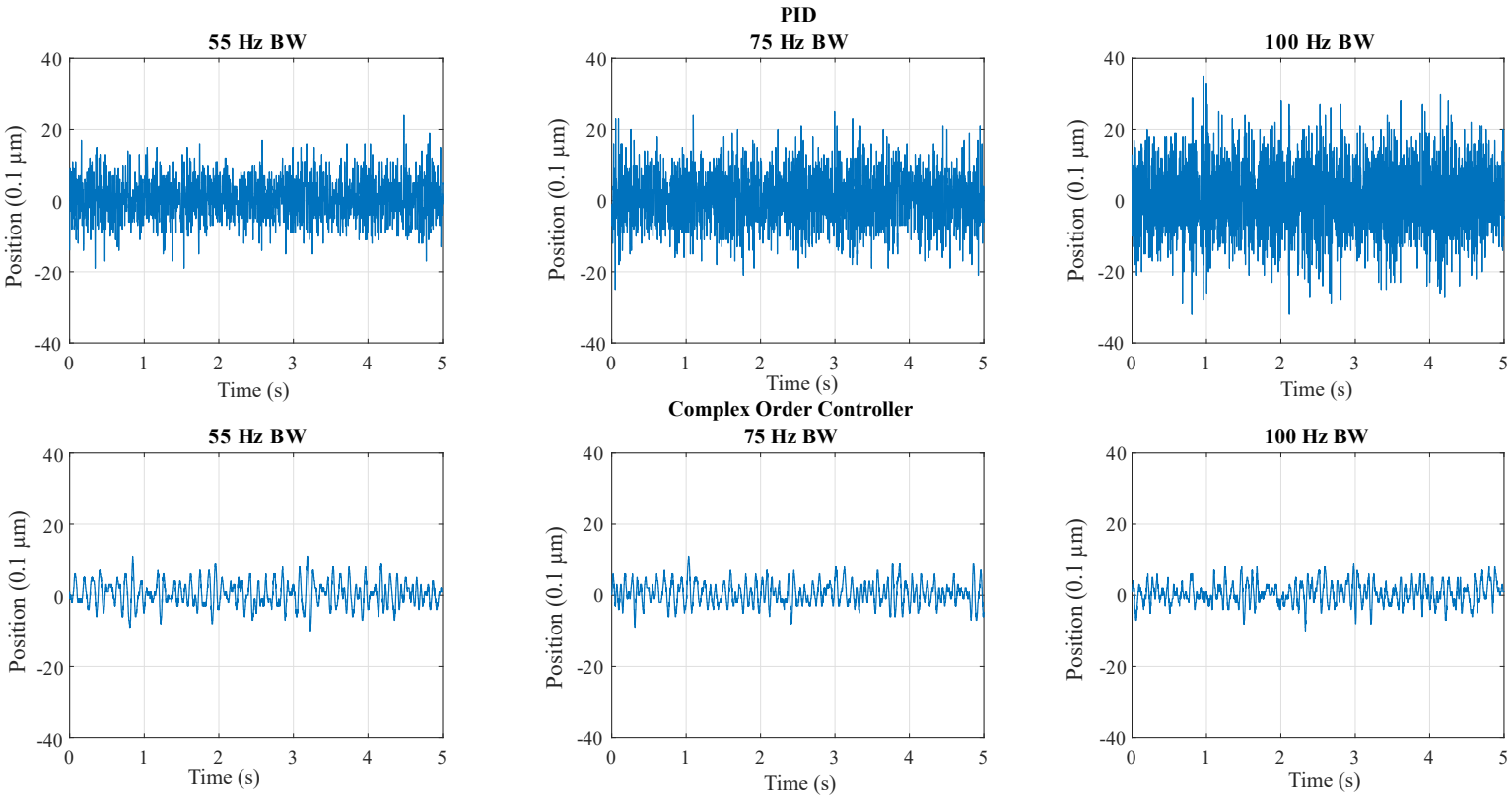

Fig. 14 System response to added noise.

Acknowledgements This work was supported by NWO, through OTP TTW project #16335, by FCT, through IDMEC, under LAETA, project UID/EMS/50022/2019, and grant SFRH/BSAB/142920/2018 attributed to the first author.

Compliance with Ethical Standards

Conflict of Interest The authors declare that they have no conflict of interest.

References

1. URL https://www.mathworks.com/matlabcentral/fileexchange/70366-complex-order-reset-controllers
2. Chen, L., Saikumar, N., HosseinNia, S.H.: Development of robust fractional-order reset control. IEEE Transactions on Control Systems Technology (2019). Http://doi.org/10.1109/TCST.2019.2913534
3. Guo, Y., Wang, Y., Xie, L.: Frequency-domain properties of reset systems with application in hard-disk-drive systems. IEEE Transactions on Control Systems Technology **17**(6), 1446–1453 (2009)
4. Moghadam, M.G., Padula, F., Ntogramatzidis, L.: Tuning and performance assessment of complex fractional-order PI controllers. In: 3rd IFAC Conference on Advances in Proportional-Integral-Derivative Control, vol. 51, pp. 757–762 (2018)
5. Moreau, X., Altet, O., Oustaloup, A.: The Crone suspension: management of the dilemma comfort–road holding. Nonlinear Dynamics **38**, 461–484 (2004)
6. Ogata, K.: Modern control engineering. Prentice Hall (2010)
7. Oustaloup, A.: La commande CRONE — commande robuste d'ordre non-entier. Hermès (1991)
8. Oustaloup, A., Bansard, M.: First generation CRONE control. In: International Conference on Systems, Man and Cybernetics. IEEE, Le Touquet (1993)
9. Oustaloup, A., Levron, F., Matthieu, B., Nanot, F.M.: Frequency-band complex noninteger differentiator: characterization and synthesis. IEEE Transactions on Circuits and Systems—I: Fundamental Theory and Applications **47**(1), 25–39 (2000)
10. Oustaloup, A., Mathieu, B., Lanusse, P.: Second generation CRONE control. In: International Conference on Systems, Man and Cybernetics. IEEE, Le Touquet (1993)
11. Palanikumar, A., Saikumar, N., HosseinNia, S.H.: No more differentiator in PID: Development of nonlinear lead for precision mechatronics. In: 17th European Control Conference, pp. 991–996 (2018)
12. Podlubny, I.: Fractional differential equations: an introduction to fractional derivatives, fractional differential equations, to methods of their solution and some of their applications. Academic Press, San Diego (1999)
13. Saikumar, N., HosseinNia, S.: Generalized fractional order reset element (gfrore). In: 9th European Nonlinear Dynamics Conference (ENOC) (2017)
14. Saikumar, N., Sinha, R.K., HosseinNia, S.H.: 'constant in gain lead in phase' element — application in precision motion control.

IEEE/ASME Transactions on Mechatronics (2019). Http://doi.org/10.1109/TMECH.2019.2909082
15. Saikumar, N., Sinha, R.K., HosseinNia, S.H.: Resetting disturbance observers with application in compensation of bounded nonlinearities like hysteresis in piezo-actuators. Control Engineering Practice **82**, 36–49 (2019)
16. Samko, S.G., Kilbas, A.A., Marichev, O.I.: Fractional integrals and derivatives. Gordon and Breach, Yverdon (1993)
17. Shah, P., Agashe, S.: Review of fractional PID control. Mechatronics **38**, 29–41 (2016)
18. Valério, D., Sá da Costa, J.: An Introduction to Fractional Control. IET, Stevenage (2013). ISBN 978-1-84919-545-4